ENHANCED PERFORMANCE OF CuIn$_{1-x}$G$_x$Se$_2$ SOLAR CELL THROUGH OPTIMIZATION OF ABSORBER AND BUFFER LAYER PROPERTIES USING SCAPS-1D[†]

Godwin J. Ibeh[a], Celine O. Lawani[a], Jayeola O. Emmanuel[b], Peter O. Oyedare[c], ⓘEli Danladi[d]*, Olumide O. Ige[a]

[a]*Department of Physics, Nigerian Defence Academy, Kaduna, Nigeria*
[b]*Department of Basic Science and General Studies, Federal College of Forestry Mechanization, Kaduna, Nigeria*
[c]*Department of Science Laboratory Technology, Federal Polytechnic Ede, Osun State, Nigeria*
[d]*Department of Physics, Federal University of Health Sciences, Otukpo, Benue State, Nigeria*
Corresponding Author: Email: danladielibako@gmail.com, tel.: +2348063307256

This study is a follow up to our previously published article on "Numerical Simulation of Copper Indium Gallium Diselenide Solar Cells Using One Dimensional SCAPS Software". Five more parameters were optimized which are: absorber band gap, absorber electron affinity, buffer layer band gap, buffer layer electron affinity and working temperature using the same simulation tool initially used. When the absorber bandgap was varied between 0.8 eV and 1.6 eV, the efficiency of the solar cell increases until it reached its peak at 27.81%. This occurred at absorber bandgap of 1.4 eV. Other photovoltaic parameters at this optimum value are: V_{oc} of 1.00 V, J_{sc} of 31.99 mA/cm^2 and FF of 87.47 %. On varying the absorber electron affinity from 4.20 eV through 4.55 eV, we obtained an optimum value of 4.45 eV at V_{oc} of 0.82 V, J_{sc} of 37.96 mA/cm^2, FF of 84.99 % and an efficiency of 26.36%. The optimization of buffer bandgap resulted in an optimal value of 3.0 eV, when the buffer bandgap was varied between 1.6 eV and 3.2 eV. The photovoltaic parameters at this optimal value are: V_{oc} of 0.80 V, J_{sc} of 37.96 mA/cm^2, FF of 85.22 % and an efficiency of 25.86%. The effect of buffer electron affinity was studied by varying its value between 4.00 eV and 4.40 eV and its best value was found to be 4.05 eV at photovoltaic parameters with a V_{oc} of 0.82 V, J_{sc} of 37.96 mA/cm^2, FF of 84.98 % and an efficiency of 26.36 %. These optimized values in all parameters were used to simulate a solar cell which resulted to device with performances: V_{oc} of 1.11 V, J_{sc} of 31.50 mA/cm^2, FF of 88.91 % and an efficiency of 31.11 %. On varying the working temperature on the optimized solar cell, the optimized device with its best performance at 270 K with Photovoltaic (PV) values of V_{oc} of 1.15 V, J_{sc} of 31.55 mA/cm^2, FF of 88.64 % and an efficiency of 32.18%. The results obtained were encouraging and can serve as a guide to those involved in practical development of solar cells.
Keywords: SCAPS, Buffer Layer, Solar cells, photovoltaic
PACS: 61.43.Bn; *68.55.ag*; *68.55.jd*; 73.25.+i; 72.80.Tm; 41.20.Cv

1. INTRODUCTION

The process of getting energy from sources like fossil fuels which has been a major source of power for most countries of the world, has been found to pose a wide range of dangers (causing health concerns, ozone layer depletion, enhanced greenhouse effect, etc.) to human existence. Considering the very important role of electrical energy in the technological advancement of the society, its demand is far greater than ever in developed and developing countries. Nations without natural deposits of oil and gas are likely to find it very difficult in the nearest future to get supplies of these products since they are expensive, fast diminishing and politically regulated [1]. A good alternative to oil and gas sources for the production of electrical energy would have been found in nuclear energy sources such as uranium and plutonium but accidents in nuclear power plants and disposal of nuclear waste are a great challenge.

The search for a renewable and clean source of energy for industrial, technological and domestic purposes has led to the ongoing efforts at exploiting energy from the sun which is known alternatively as solar energy. Over the years, researchers have been finding the most efficient ways to harness solar energy and this has led to the development of the solar cell. In order to be able to understand the operation of solar cells, numerical modeling has been used in a number of instances and it has proven to be a very important tool in this regard [2,3].

As a follow up to our previously published article [3], we made use of SCAPS to optimize additional five parameters which include: absorber band gap, absorber electron affinity, buffer layer band gap, buffer layer electron affinity and working temperature.

2. DEVICE MODELLING AND SIMULATION

In line with the initial device set up demonstrated in our previous work [3], we utilized a solar capacitance simulation software based on the poisson and continuity equation to achieve the desired objective. The details of the set-up and simulation can be obtained in Lawani et al. [3]. In this study, similarly, a defect from double acceptor with a gaussian energy distribution, value of concentration of $1.0E + 14$ cm^{-3} defect, and level of energy of 0.1, 0.4, eV slightly above valence band, were introduced into the CIGS (absorber) layer. The defect can be seen to arise as a result of Cu$_{III}$ defect

which is most times noticed in CIGS absorbers [4]. The absorber band gap was varied from 0.8 – 1.6 eV, absorber electron affinity was varied from 4.20 – 4.55 eV, buffer layer band gap was varied from 1.6 – 3.2 eV, buffer layer electron affinity was varied from 4.00 – 4.40 eV. The simulated device structure is as shown in Fig 1. All other parameters were kept constant while varying the aforementioned parameters.
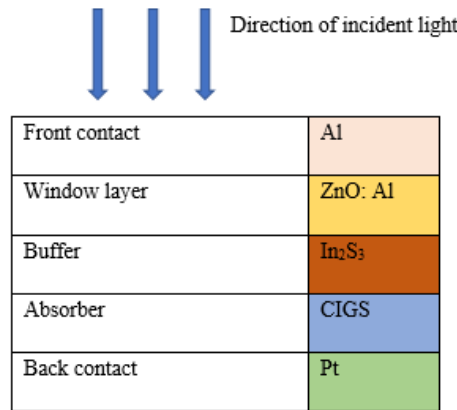
Direction of incident light

Front contact	Al
Window layer	ZnO: Al
Buffer	In₂S₃
Absorber	CIGS
Back contact	Pt

Figure 1. Model of the simulated solar cell [3]

3. RESULTS AND DISCUSSION
3.1. Effect of varying CIGS (absorber) bandgap

The effect of absorber band gap was investigated by varying the CIGS layer band gap from 0.8 eV through 1.6 eV. Figure 2 shows the variation of CIGS solar cells' photovoltaic parameters with increasing absorber layer bandgap.
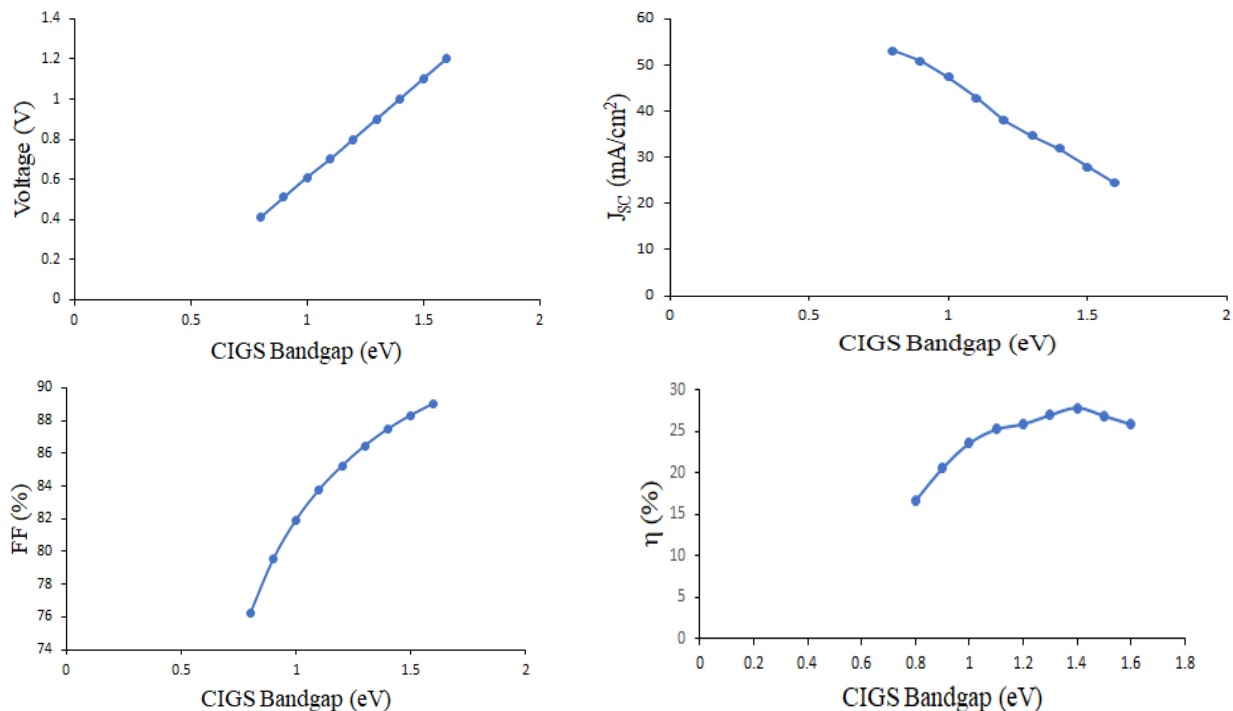
Figure 2. Variation of Voc, Jsc, FF and η with increasing CIGS bandgap

It was observed that J_{SC} decreased with increasing bandgap energy. This decrease occurs because part of the solar spectrum was not harvested by the solar cells [5]. An absorber with high bandgap energy absorbs photons with low wavelengths to release electrons from the valence band to conduction band in accordance with Einstein's equation [6,7] given in equation 1 below:

$$E_g = \frac{hc}{\lambda_g},$$ (1)

where h is Plank's constant, c is the velocity of light and λ_g are wavelength which matches the band gap of the absorber. V_{OC} is seen to increase with increasing bandgap of the absorber.

According to Scheer and Schock [8], decreasing the bandgap of the absorber increases photocurrent but causes a decrease in V_{OC}. This is clear when the relationship between V_{OC} and bandgap in equation 2 is considered.

$$V_{OC} = \frac{E_a}{q} + \frac{AKT}{q} \ln\left(-\frac{J_{SC}\,\eta(V_{OC})}{J_{00}}\right) \qquad (2)$$

where A is the solar cells' quality factor, q is the elementary charge, E_a is the activation energy of J_O (and is approximately equal to the absorber bandgap [8]), J_O is saturation current density and J_{00} is the reference current density of the solar cell.

The observed increase in efficiency is due to the increase in V_{OC} and fill factor [9], but as the J_{SC} drops with increasing bandgap of absorber, the efficiency begins to fall since light absorption reduces. This is detrimental to the solar cells as their performance goes down. Table 1 gives the dependence of the solar cells' performance on CIGS layer bandgap. It shows that the highest efficiency achieved after variation of CIGS absorber band gap is 27.81 % and this occurred at a bandgap of 1.4 eV. Other photovoltaic parameters at this optimized value of band gap are: V_{OC} of 1.0 V, J_{SC} of 31.99 mA/cm^2 and FF of 87.47 %.

Table 1. Dependence of solar cells' performance on absorber layer bandgap

CIGS bandgap (eV)	V_{OC}(V)	J_{SC}(mA/cm^2)	FF (%)	η (%)
0.8	0.41	53.13	76.20	16.55
0.9	0.51	50.83	79.51	20.50
1.0	0.61	47.43	81.92	23.52
1.1	0.70	42.86	83.76	25.22
1.2	0.80	37.96	85.22	25.85
1.3	0.90	34.76	86.45	26.94
1.4	1.00	31.99	87.47	27.81
1.5	1.10	27.86	88.31	26.82
1.6	1.20	24.45	89.02	25.82

The J-V curves in Figure 3(a) show that as bandgap of the absorber increases, the Jsc of the solar cells decreases but the open circuit voltage increases. Figure 3(b) depicts the QE as a function of wavelength for corresponding CIGS layer bandgap. For device with wavelength within the range 300 nm – 1600 nm the absorption efficiency remains the same.

The arrangement of the curves (curves corresponding to lower bandgaps are outermost, while those curves corresponding to higher bandgaps are innermost) show the inverse relationship existing between the various bandgaps and their corresponding wavelengths, as given in Equation 1.
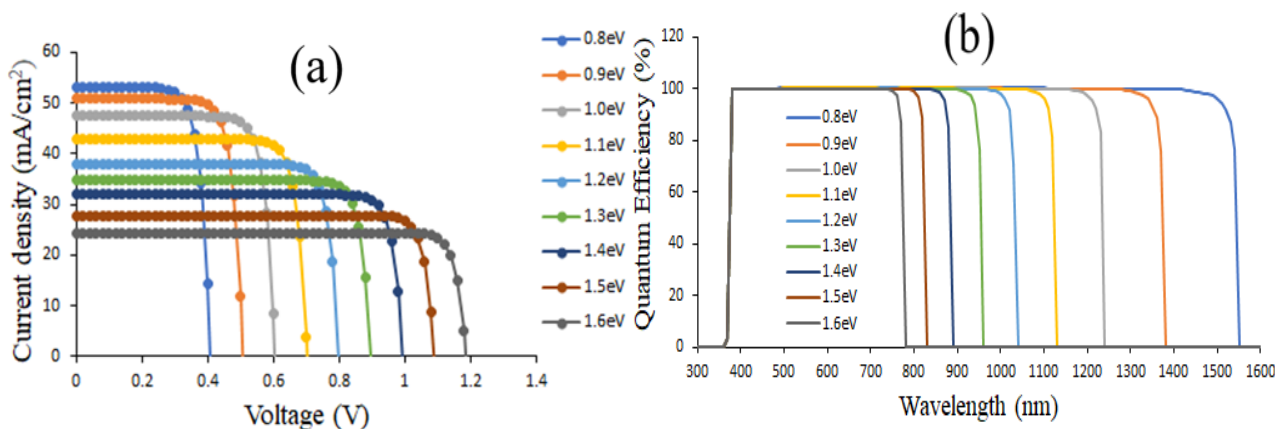
Figure 3. (a) J-V curves and (b) QE of CIGS solar cell with various values of absorber layer bandgap

3.2. Effect of varying electron affinity of CIGS (absorber) layer

Table 2 shows the dependence of solar cells' performance on electron affinity. In the case where the electron affinity of the n-type layer is smaller than that of the p-type layer, a positive conduction band offset (also known as a spike) given in equation 3 is formed otherwise a cliff is formed [10]

$$\Delta E_C = E_{C,n} - E_{C,P} > 0, \qquad (3)$$

where $E_{C,n}$ is conduction band energy for n-type layer and $E_{C,P}$ is conduction band energy for p-type layer.

From Table 2, V_{OC} increases until it saturates at a bandgap of 4.35 eV (Figure 4). The increase in V_{OC} is very likely caused by a spike which reduces the occurrence of recombination (This is good for the solar cells as recombination degrades their performance.). This also explains the rise in efficiency of the CIGS solar cells as electron affinity of absorber increases. J_{SC} remains constant but fill factor rises to its optimum value and begins to fall due to the formation

of high spikes [11]. The optimum value of electron affinity for the absorber was found to be 4.45 eV and the metric parameters are: V_{OC} of 0.82 V, J_{SC} of 37.96 mA/cm^2, FF of 84.99 % and a PCE of 26.36 %.
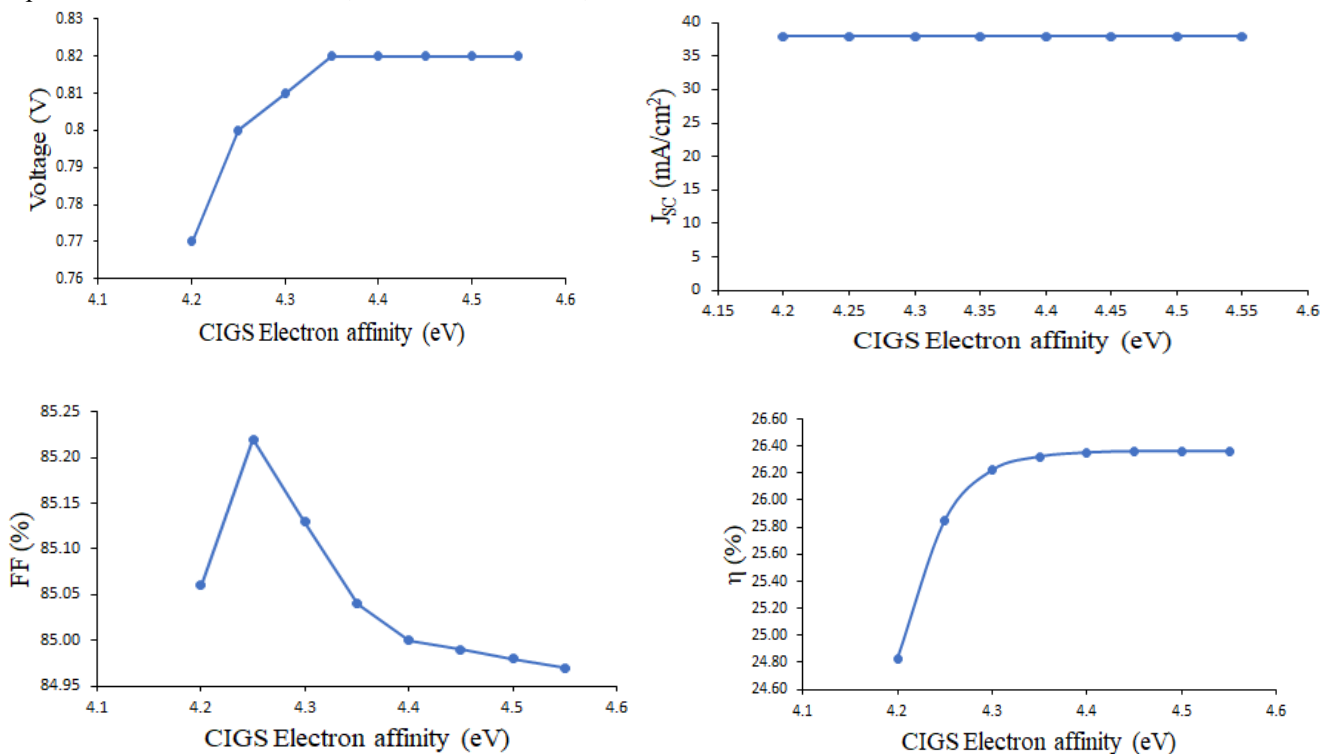

Figure 4. Variation of Voc, Jsc, FF and η with increasing CIGS Electron Affinity

Table 2. Dependence of solar cells' performance on electron affinity of absorber layer

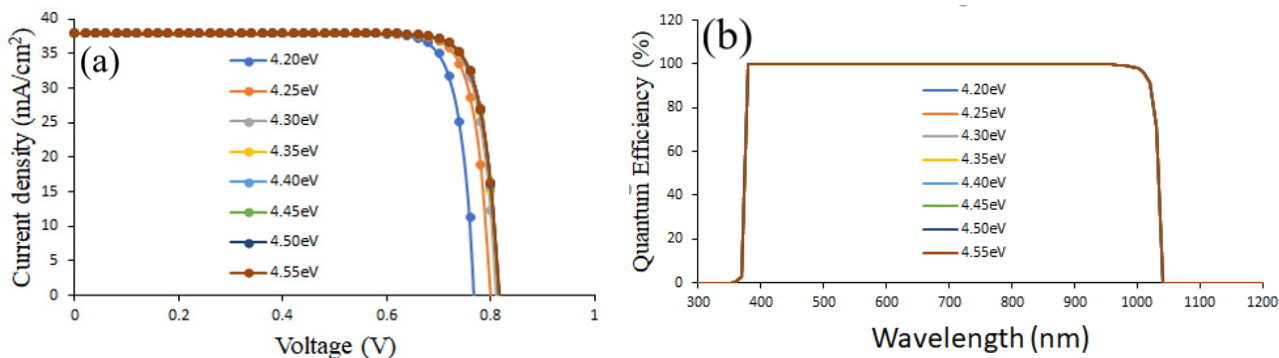| CIGS electron affinity (eV)	Voc (V)	Jsc (mA/cm^2)	FF (%)	η (%)
4.20	0.77	37.96	85.06	24.83
4.25	0.80	37.96	85.22	25.85
4.30	0.81	37.96	85.13	26.22
4.35	0.82	37.96	85.04	26.32
4.40	0.82	37.96	85.00	26.35
4.45	0.82	37.96	84.99	26.36
4.50	0.82	37.96	84.98	26.36
4.55	0.82	37.96	84.97	26.36

Figure 5. (a) J-V curves and (b) QE of CIGS solar cell with various values absorber (CIGS) electron affinity

The J-V curves in Fig. 5(a) show that for all values of electron affinity of absorber, J_{SC} remains the same while V_{OC} increased until it attained its optimum value and remained constant (this is shown in areas where the curves overlap). Figure 5(b) is the representation of QE as a function of wavelength for the selected values of CIGS electron affinity.

As demonstrated, within the wavelength range of 300 nm – 1200 nm, an overlap in the QE curves was observed which is attributed to the unchanged absorption efficiency within the selected values of the CIGS electron affinity. This

spectral response proves that absorber (CIGS) electron affinity has only a slight effect on the metric parameter of CIGS solar cells investigated.

3.3. Effect of varying In$_2$S$_3$ (buffer) bandgap

Figure 6 shows the variation of photovoltaic parameters with buffer layer bandgap. The buffer bandgap was varied from 1.6 eV through 3.2 eV.
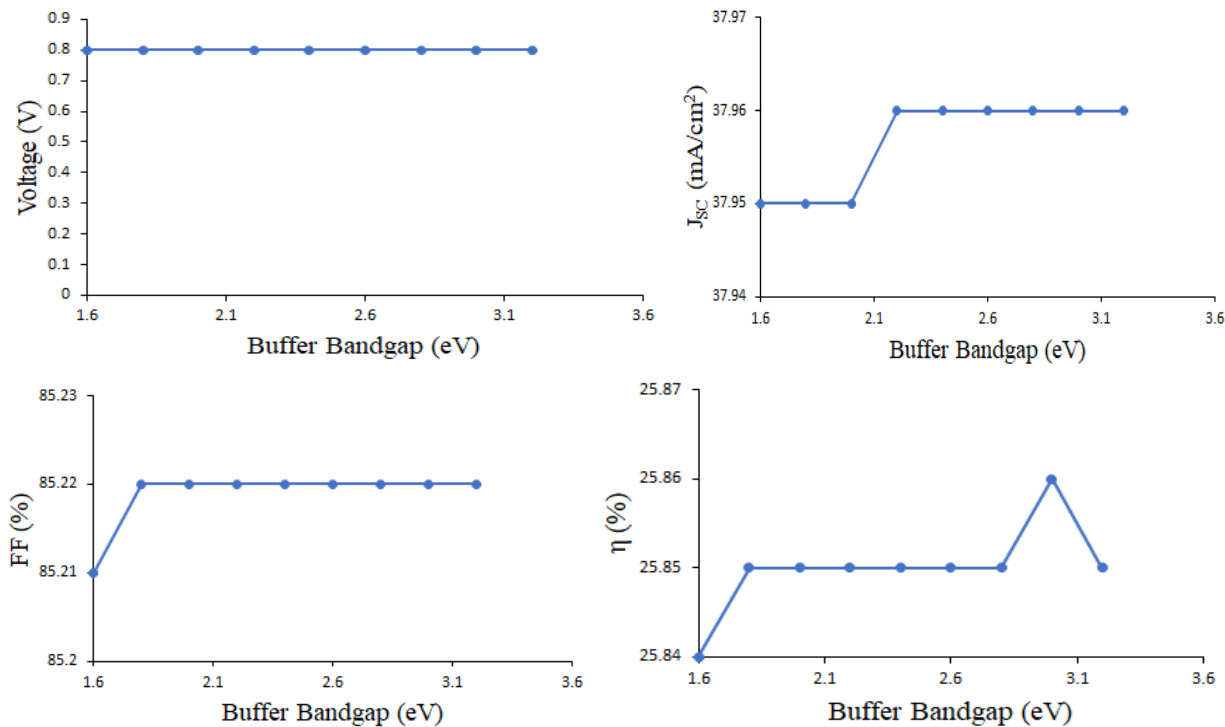

Figure 6. Variation of Voc, Jsc, FF and η with increasing CIGS Electron Affinity

It was discovered that while V$_{OC}$ was unaffected by this variation, J$_{SC}$ and FF rose to their peaks and remained constant thereafter. The efficiency also rose to its optimum value and then dropped. Although J$_{SC}$ remained constant for higher values of buffer bandgap, it increased initially with an increase in buffer layer bandgap because more photons were allowed to reach the absorber layer and create more electron-hole pairs [12]. This translates to an increase in efficiency and fill factor but efficiency eventually drops beyond buffer bandgap of 3.0 eV because as bandgap goes higher, photons cannot achieve the needed amount of energy to create enough electron-hole pairs [13] which is needed to increase efficiency. The performance of the solar cells then drops. The best value of buffer bandgap after optimization is 3.0 eV and this occurs at V$_{OC}$ of 0.80 V, J$_{SC}$ of 37.96 mA/cm^2. FF of 85.22 % and efficiency of 25.86 % (see Table 3).

Table 3. Dependence of solar cells' performance on buffer layer bandgap

Buffer bandgap(eV)	Voc (V)	Jsc (mA/cm2)	FF (%)	η (%)
1.6	0.80	37.95	85.21	25.84
1.8	0.80	37.95	85.22	25.85
2.0	0.80	37.95	85.22	25.85
2.2	0.80	37.96	85.22	25.85
2.4	0.80	37.96	85.22	25.85
2.6	0.80	37.96	85.22	25.85
2.8	0.80	37.96	85.22	25.85
3.0	0.80	37.96	85.22	25.86
3.2	0.80	37.96	85.22	25.85

Figure 7(a) shows the curves for short circuit current density against the open circuit voltage for the different values of buffer bandgap used in this study. It reveals overlapping curves and these overlaps are more prominent as the curves drop to meet the voltage axis. This means that while J$_{SC}$ experiences slight variations, V$_{OC}$ remains constant for all values of buffer layer band gap.

Figure 7(b) is a representation of the QE versus wavelength for the selected values of buffer (In$_2$S$_3$) layer bandgap. Selecting the range of wavelength to be 300 nm – 1200 nm, results to spectral overlap. We therefore speculate that In$_2$S$_3$ layer bandgap has negligible or no effect on the performance of CIGS solar cells studied.
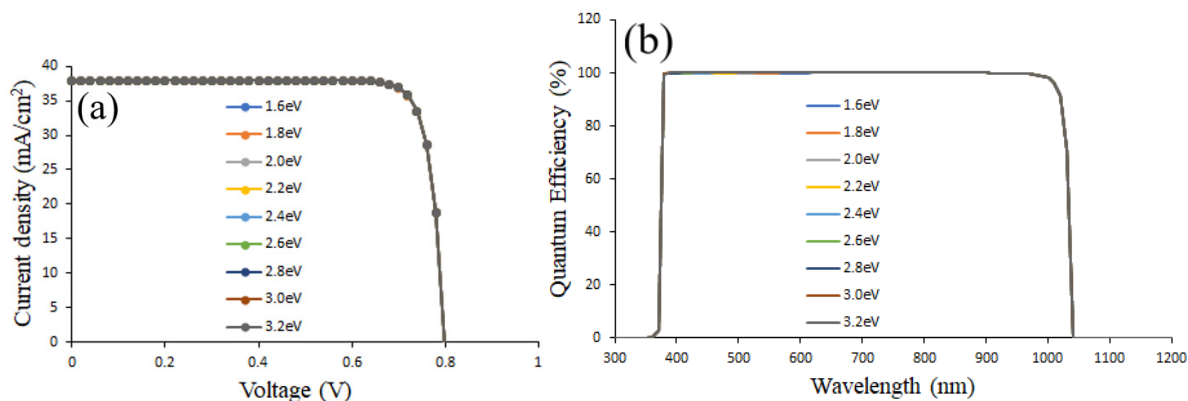
Figure 7. (a) J-V curves and (b) QE of CIGS solar cell with different values of buffer (In_2S_3) layer bandgap.

3.4 Effect of varying electron affinity of In_2S_3(buffer) layer

Figure 8 shows the variation of photovoltaic parameters with an increase in the electron affinity of the buffer layer. J_{SC} is observed to be constant until it experiences a slight increase beyond an electron affinity of 4.4 eV.
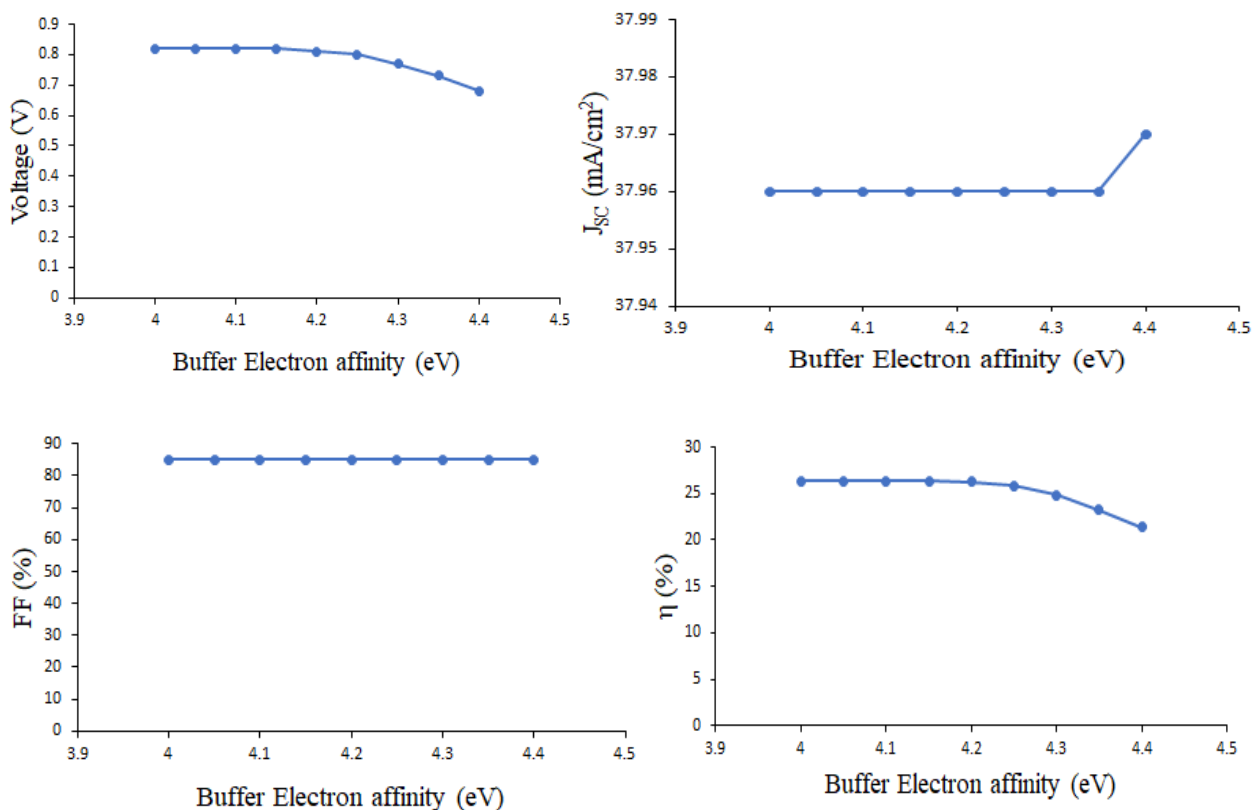

**Figure 8.** Variation of Voc, Jsc, FF and η with increasing electron affinity of buffer layer

This is due to the formation of cliffs which pose no barrier to photogenerated electrons. This would have been good for the solar cells' performance but as a cliff helps to boost Jsc it causes recombination between electrons injected from buffer layer and the interface defects [11]. We therefore see that V_{OC}, and efficiency, begin to decrease while fill factor remains unchanged. After optimization, the best value of buffer electron affinity is seen to be 4.05 eV at V_{OC} of 0.82 V, J_{SC} of 37.96mA/cm^2, FF of 84.98 % and efficiency of 26.36 % as shown in Table 4.

The J-V curves (Figure 9(a)) show that between buffer electron affinities of 4.00 eV and 4.15 eV, the open circuit voltage is the same but it varies thereafter, with the curve for the highest electron affinity appearing innermost (this indicates that the open circuit voltage is least for the highest electron affinity). The short circuit current density shows little or no change.

Figure 9(b) depict the QE versus wavelength of electron affinity values selected for buffer layer (In_2S_3). Choosing within a range of 4.00 eV and 4.15 eV, there is a clear overlap in the QE curves.

Table 4. Dependence of solar cells' performance on electron affinity of buffer layer

In$_2$S$_3$ electron affinity (eV)	Voc(V)	Jsc(mA/cm2)	FF(%)	η (%)
4.00	0.82	37.96	84.98	26.36
4.05	0.82	37.96	84.98	26.36
4.10	0.82	37.96	84.98	26.35
4.15	0.82	37.96	84.98	26.32
4.20	0.81	37.96	84.98	26.22
4.25	0.80	37.96	84.98	25.85
4.30	0.77	37.96	84.98	24.83
4.35	0.73	37.96	84.98	23.24
4.40	0.68	37.97	84.98	21.40
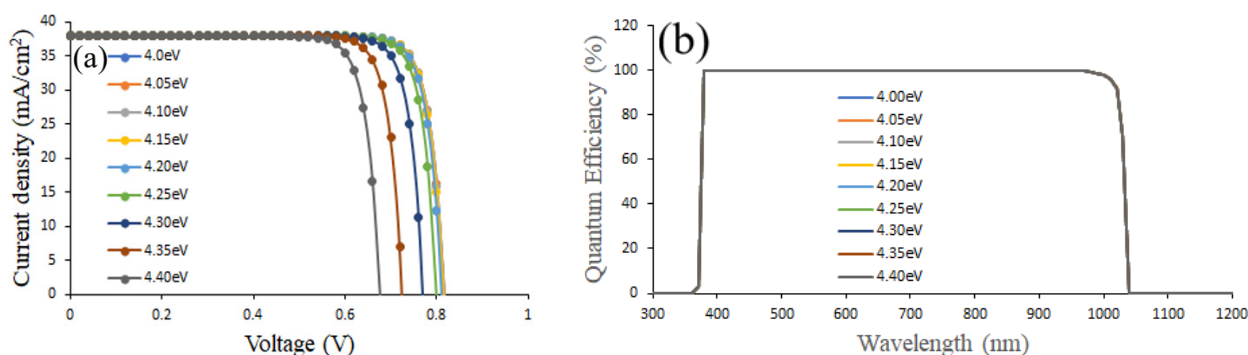
Figure 9. (a) J-V curves and (b) QE of CIGS solar cell different values of buffer (In$_2$S$_3$) layer electron affinity

3.5 Performance of optimized parameters

In accordance to the optimized parameters obtained in this research and those sourced from our previous work [3] (see Table 5), an efficiency of 31.13 %, current density of 31.55 mA/cm^3, voltage of 1.11 V and fill factor of 88.91 % were obtained (see Figure 10 and Table 6). These photovoltaic parameters obtained from optimization agree very much with those of the theoretical limits quoted by Ruhle [14]. Compared with the experimental data obtained in literature [15], which shows a PCE value of 22.6 %, the optimized device in this work demonstrates an enhanced value of ~37.74 % in PCE over the reported [15].

Table 5. Optimized parameters of the device

Optimized parameters	Absorber	Buffer
Multivalent defect density(cm^{-3})	1E + 10 [3]	----
Thickness (μm)	1.20 [3]	0.01[3]
Bandgap(eV)	1.40	3.00
Electron affinity (eV)	4.45	4.05

Table 6. photovoltaic parameters corresponding to optimized parameters of the CIGS solar cells compared with those of experimental researches and the maximum theoretical limit for solar cells with absorber bandgap of 1.4 eV

| Simulation	V$_{OC}$ (V)	J$_{SC}$ (mA/cm^2)	FF (%)	η (%)
Initial	0.79	37.96	85.22	25.85
Optimized multivalent defect density (cm^{-3})	0.82	37.96	86.04	26.81
Optimized absorber thickness (**μ**m)	0.81	37.75	85.27	25.94
Optimized absorber bandgap(eV)	1.00	31.99	87.47	27.81
Optimized electron affinity of absorber (eV)	0.82	37.96	84.99	26.36
Optimized buffer thickness (**μ**m)	0.80	37.96	85.23	25.98
Optimized buffer bandgap (eV)	0.80	37.96	85.22	25.86
Optimized electron affinity of buffer (eV)	0.82	37.96	84.98	26.36
Final optimization	1.11	31.55	88.91	31.13
Maximum theoretical (Shockley-Queisser) limit	1.12	32.88	89.30	32.91 [14]
Experimental data	0.76	34.80	79.10	20.80 [16]
Experimental data	0.74	36.70	80.50	22.00 [17]
Experimental data	0.74	37.80	80.60	22.60 [15]
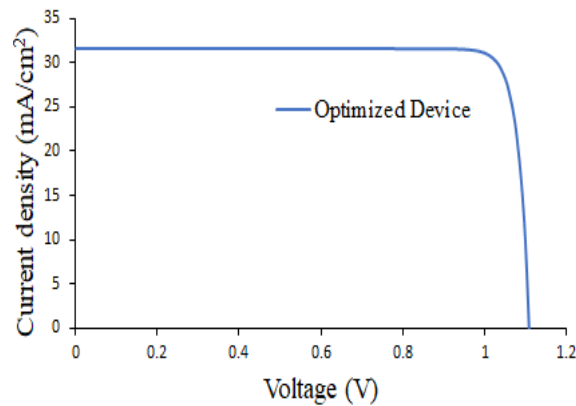
Figure 10. J-V curve of CIGS solar cell with optimized parameters

3.6 Effect of working temperature on the optimized device

Solar panels are usually installed in an open environment [18] and so the temperature under which they operate could affect their performance. When sunlight falls on solar cells, their temperatures rise. In this research the working temperature of the optimized cell was varied from 260 K through 340 K. Table 7 shows the dependence of solar cells performance on working temperature while Figure 11 gives the variation of photovoltaic parameters with increasing temperature. J_{SC} remains constant (Figure 11(b)) but V_{OC} keeps decreasing because of an increase in reverse saturation current with temperature. The fill factor reaches its peak at a temperature of 280 K and then begins to drop. This fall is due to light induced degradation [19]. The efficiency attains its optimum value at 270 K and also drops because when operating temperatures get higher than this optimum value, the electrons in the solar cell gain energy but instead of boosting electricity generation, they become unstable and recombine before they are collected [20]. Figure 12 shows the J-V curves of the CIGS solar cells with increasing temperature.

Table 7. Dependence of optimized solar cells' performance on temperature

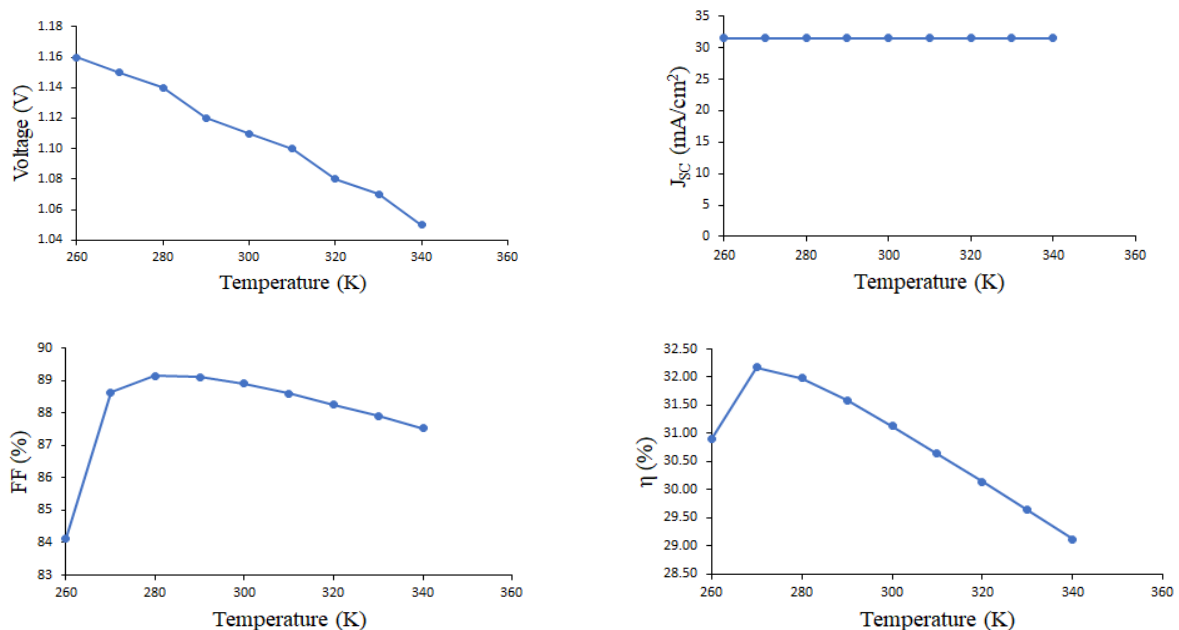| Temperature (K)	V_{OC} (V)	J_{SC} (mA/cm^3)	FF (%)	η (%)
260	1.16	31.55	84.14	30.90
270	1.15	31.55	88.64	32.18
280	1.14	31.55	89.14	31.98
290	1.12	31.55	89.11	31.59
300	1.11	31.55	88.91	31.13
310	1.10	31.55	88.60	30.64
320	1.08	31.55	88.25	30.14
330	1.07	31.55	87.90	29.64
340	1.05	31.55	87.52	29.12

Figure 11. Variation of Voc, Jsc, FF and η with increasing temperature
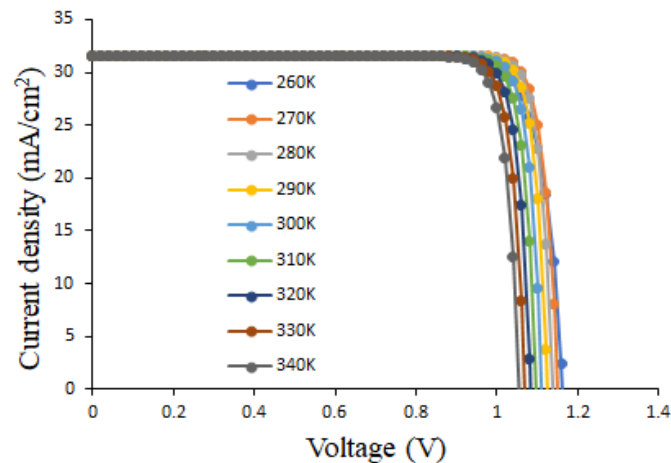
Figure 12. J-V curves of CIGS solar cells with increasing temperature

4. CONCLUSION

This research work investigated the influence of absorber bandgap, absorber layer electron affinity, buffer bandgap and buffer electron affinity by means of SCAPS simulation. The efficiency of the initial device which was set up in line with our previous work yielded an efficiency of 25.85% and on optimization of the aforementioned parameters, optimal values of 1.4 eV, 4.45 eV, 3.0 eV and 4.05 eV respectively, were obtained. These values were used together with optimum values of multivalent defect density (1E + 10 cm^{-3}) in absorber, absorber layer thickness (1.2µm) and buffer layer thickness (0.01 µm) obtained in our previously published work, to simulate a solar cell which turned out to be the best device having photovoltaic parameters with a V$_{OC}$ of 1.11 V, J$_{SC}$ of 31.55 mA/cm^2, fill factor of 88.91 %. and efficiency of 31.13 %. Except for J$_{SC}$, these values are higher than those obtained in our paper, where the best device had photovoltaic parameters with V$_{OC}$ of 0.83 V, J$_{SC}$ of 37.75 mA/cm^2, fill factor of 86.26 % and an efficiency of 27.00 %. This clearly shows that the cumulative effect of optimizing more parameters of the absorber and buffer layer produces better performing solar cells (as three parameters were used to produce the optimized solar cell in our former paper whereas in this work, seven were used). Lastly, the effect of working temperature on the optimized solar cell was investigated. The study showed that the best performance of the optimized device was achieved at 270 K and the photovoltaic parameters corresponding to this optimum working temperature are; V$_{OC}$ of 1.15 V, J$_{SC}$ of 31.55 mA/cm^2, FF of 88.64 % and an efficiency of 32.18 %. At 270 K, this best device would work optimally in cold countries of the world like Russia and Canada were temperatures can get as low as 268 K.

ORCID IDs

Eli Danladi, https://orcid.org/0000-0001-5109-4690

REFERENCES

[1] O.I. Okoro, and T.C. Madueme, Nigerian Journal of Technology, **23,** 58 (2004). https://www.ajol.info/index.php/njt/article/view/123333/112876
[2] B. Padmanabham, Master's Degree Thesis, Arizona state University (2008).
[3] C.O. Lawani, G.J. Ibeh, O.O. Ige, E. Danladi, J.O. Emmanuel, A.J. Ukwenya, and P.O. Oyedare, Journal of the Nigerian Society of physical Sciences, **3**, 48 (2021). https://doi.org/10.46481/jnsps.2021.333
[4] S. Wei, S. Zhang, and A. Zunger, "Effects of Ga addition to CuInSe$_2$on its electronic, structural and defect properties", Applied Physics letters, **72,** 3199, (1998). http://dx.doi.org/10.1063/1.121548
[5] G. Hanna, A. Jasenek, U. Rau, and H.W. Schock, Thin Solid Film, **387,** 71 (2001). https://doi.org/10.1016/S0040-6090(00)01710-7
[6] C. Daniella, F. Popescu, P. Joan, and V. Andrei, Procedia-Social and Behavioural Sciences, **191,** 512 (2015). https://doi.org/10.1016/j.sbspro.2015.04.284
[7] C. Liu, and W. Liu, Optik, **127,** 7359-7366, (2016). https://doi.org/10.1016/j.ijleo.2016.05.045
[8] R. Scheer, and H. Schock, *Solar Energy & Photovoltaics*, (John Wiley & Sons, Inc., 2011), pp. 384.
[9] Z. Mohammadi, Journal of Fundamental and Applied Sciences, **8**, 935 (2016). https://doi.org/10.4314/jfas.v8i3s.114
[10] L. Puyvelde, Doctoral dissertation, Ghent university, Belgium (2015).
[11] A. Sylla, S. Toure, and J. Vilcot, International Journal of Science and Research, **6**, 855-860, (2015).
[12] M.I. Hossain, P. Chelvanathan, M. Zaman, M. Karim, M. Alghoul, and N. Amin, Chalcogenide Letters, **8**, 315-324, (2011). http://chalcogen.ro/315_Hossain.pdf

[13] M. Green, *Eagle Cliffs*, (Prentice Hall, 1982).
[14] S. Ruhle, Solar Energy, **130**, 139 (2016). https://doi.org/10.1016/j.solener.2016.02.015
[15] P. Jackson, R. Wuerz, D. Hariskos, E. Lotter, W. Witte, and M. Powalla, Physica Status Solidi, **10**, 583 (2016). https://doi.org/10.1002/pssr.201600199
[16] P. Jackson, D. Hariskos, R. Wuerz, W. Wischmann, and M. Powalla, Physica Status Solidi, **8**, 219-222, (2014). https://doi.org/10.1002/pssr.201409040
[17] ZWS, ZSW-CIGS22Percent-en.pdf (2016). https://www.zsw-bw.de/fileadmin/user_upload/PDFs/Pressemitteilungen/2016/pi07-2016-ZSW-CIGS22Percent-en.pdf
[18] K. Sobayel, K.S. Rahman, M.R. Karim, M.O. Aijaz, M.A. Dar, M.A. Shar, H. Misran, and N. Amin, Chalcogenide Letters, **15**, 333-340, (2018). https://chalcogen.ro/307_SobayelK.pdf
[19] M. Green, Progress in Photovoltaic Research and Application **11**, 333-340, (2003). https://doi.org/10.1002/pip.496
[20] P. Chelvanatan, M.I. Hossain, and N. Amin, Current applied physics, **10**, S387-S391, (2010). https://doi.org/10.1016/j.cap.2010.02.018

<div align="center">

ПОКРАЩЕНА ПРОДУКТИВНІСТЬ СОНЯЧНОЇ БАТАРЕЇ CuIn$_{1-x}$G$_x$Se$_2$ ЗАВДЯКИ ОПТИМІЗАЦІЇ ВЛАСТИВОСТЕЙ АБСОРБЕРА ТА БУФЕРНОГО ШАРУ ЗА ДОПОМОГОЮ SCAPS-1D

</div>

<div align="center">

Годвін Дж. Ібе[a], Селін О. Лавані[a], Джасола О. Еммануель[b], Пітер О. Ойедаре[c], Елі Данладі[d], Олуміде О. Іге[a]
[a]Фізичний факультет Нігерійської оборонної академії, Кадуна, Нігерія.
[b]Відділ фундаментальних наук і загальних досліджень, Федеральний коледж механізації лісового господарства, Кадуна, Нігерія
[c]Департамент наукових лабораторних технологій, Федеральна політехніка Еде, штат Осун, Нігерія
[d]Фізичний факультет, Федеральний університет наук про здоров'я, Отукпо, штат Бенуе, Нігерія

</div>

Це дослідження є продовженням нашої раніше опублікованої статті на тему «Чисельне моделювання сонячних елементів із диселеніду міді, індій-галію з використанням одновимірного програмного забезпечення SCAPS». Було оптимізовано ще п'ять параметрів, а саме: ширину забороненої зони поглинача, спорідненість до електронів поглинача, ширину забороненої зони буферного шару, спорідненість до електронів буферного шару та робочу температуру за допомогою того самого інструменту моделювання, який використовувався спочатку. Коли ширина забороненої зони поглинача змінювалася між 0,8 еВ і 1,6 еВ, ефективність сонячної батареї зростала, поки не досягла свого піку в 27,81 %. Це сталося при ширині забороненої зони поглинача 1,4 еВ. Інші фотоелектричні параметри при цьому оптимальному значенні: V$_{oc}$ 1,00 В, J$_{sc}$ 31,99 мА/см^2 і FF 87,47 %. Змінюючи спорідненість до електронів поглинача від 4,20 еВ до 4,55 еВ, ми отримали оптимальне значення 4,45 еВ при V$_{oc}$ 0,82 В, J$_{sc}$ 37,96 мА/см^2, FF 84,99 % і ефективність 26,36 %. Оптимізація ширини забороненої зони буфера призвела до оптимального значення 3,0 еВ, коли ширина забороненої зони буфера змінювалася між 1,6 еВ і 3,2 еВ. Фотоелектричні параметри при цьому оптимальному значенні: V$_{oc}$ 0,80 В, J$_{sc}$ 37,96 мА/см^2, FF 85,22 % і ККД 25,86 %. Вплив буферної електронної спорідненості досліджували, варіюючи його значення між 4,00 еВ і 4,40 еВ, і було встановлено, що його найкраще значення становить 4,05 еВ при фотоелектричних параметрах з V$_{oc}$ 0,82 В, J$_{sc}$ 37,96 мА/см^2, FF 84,98 % і ККД 26,36 %. Ці оптимізовані значення всіх параметрів були використані для моделювання сонячної батареї, що призвело до пристрою з характеристиками: V$_{oc}$ 1,11 В, J$_{sc}$ 31,50 мА/см^2, FF 88,91 % і ККД 31,11 %. Змінюючи робочу температуру оптимізованої сонячної батареї, оптимізований пристрій має найкращу продуктивність при 270 K із фотоелектричними (PV) значеннями V$_{oc}$ 1,15 В, J$_{sc}$ 31,55 мА/см^2, FF 88,64 % і ефективністю 32,18 %. Отримані результати були обнадійливими і можуть служити керівництвом для тих, хто бере участь у практичних розробках сонячних елементів.
Ключові слова: SCAPS, буферний шар, сонячні елементи, фотоелектричні